Supplementing Information

Determination of RNA concentration with FCS

We fitted FCS data with an autocorrelation function that describes a two-dimensional diffusion model:

$$G(t) = \frac{1}{N(1 + (\frac{4Dt}{\omega^2}))}$$

where D is the diffusion coefficient of the fluorescent molecules, t is the time variable, and ω is the radius of the detection volume in the experimental configuration. 1/N is the amplitude of the autocorrelation function at the y-intercept and is the inverse of the number of molecules (N) in the detection volume.

The radius of the FCS probed volume calibrated with 44nm fluorescent beads was calculated to be ~ 0.19 μm. The FCS probed volume was calculated to be ~ 0.045 fl in a living cell. One MS2-GFP molecule in the detection volume within a living bacterium represents a concentration of 37nM.

From in vivo titration experiments, the diffusion half-times of free and fully bound MS2-GFP to ms2-RNA in a living cell were found to be 1.4 +/- 0.5 ms and 30 +/- 3 ms, respectively (1).

To determine the fraction of free and ms2-RNA bound MS2-GFP proteins, we fit the autocorrelation functions with:

$$G(t) = \frac{1}{N} \times \frac{1}{[(1-y) + Qy]^2} \times \left\{ \frac{(1-y)}{(1 + \frac{t}{\tau_{free}})} + \frac{Q^2 y}{(1 + \frac{t}{\tau_{bound}})} \right\}$$

where y, the only fit parameter, is the fraction of bound MS2-GFP. ζ_{free} and ζ_{bound} are the known diffusion times of free and ms2-RNA bound MS2-GFP proteins, respectively. And the factor Q is the ratio of fluorescence intensity of bound to free MS2-GFP molecules. Q is equal to two in our experiment as two MS2-GFP homodimers are bound to one ms2-RNA transcript.

In order to derive RNA concentration, we multiply the fraction of bound MS2-GFP at any given time with the total number of MS2-GFP molecules (No) measured at the initial time-point (0 seconds) (Supplementing Figure 2). We assume that the MS2-GFP concentration within a cell remains constant during FCS measurements. In dividing cells, we induced transcription from acrAB promoter after the first cell division on surface. After the second cell division, we reduced the initial number of MS2-GFP molecules N_o by the ratio of body lengths of daughter to mother cells.

The errors in estimating RNA concentration are calculated using the equation (δy/y + δNo/No)[RNA], where δy and δNo are the fitting errors of the fraction bound and of the initial MS2-GFP concentration inside the detection volume, respectively.

Computer Simulation

In this section we describe a simple kinetic model of the time evolution of the concentration of induced RNA following a step increase in inducer concentration. We consider the condition in which the cells do not divide. The main assumptions are as follows: (i) The equilibrium of the intracellular concentration of aTc with the external concentration following induction is instantaneous. For simplicity, we hypothesize that immediately after induction the effective efflux of aTc is constant with rate μ. (ii) After induction, we assume that transcription and aTc efflux occur on longer time scales than repression and induction of the Tet promoter. This latter condition allows us to use quasi-equilibrium approximations for the repression and induction kinetics (Figure 4A).

The intracellular concentration of RNA obeys the following equation

$$\frac{\partial}{\partial t} RNA(t) = \varsigma\, P(t)\, D_{tot} - \gamma\, RNA(t) \tag{1}$$

where D_{tot} is the total concentration of plasmids, ζ is the rate of transcription and γ is the rate of RNA degradation. P is the probability that the two operator sites on the promoter region are free of Tet repressors. Integration yields the time evolution of *RNA* as function of *P(t)*:

$$RNA(t) = RNA_0\; e^{-\gamma t} + \varsigma\, D_{tot} \int_0^t P(s)\, e^{-\gamma(t-s)} ds \tag{2}$$

RNA_0 is the intracellular concentration of RNA before induction (*t<0*).

The reactions associated with the repression and induction of the *tet* promoter are depicted in Figure 4A. The Tet repressor (*R*) binds as a dimmer the two operator sites (O_1 and O_2). This binding is not cooperative and has a high affinity (Supplementing Table 1). Each Tet dimmer *R* can bind non-cooperatively two inducer molecules (*T)*. When aTc (*T*) is bound to the Tet repressor, it lowers the affinity of *R* for the operator site.

We calculate *R* and *P* as function of *T* using the condition of quasi-equilibrium for repression/induction reactions (Figure 4A) and the conservation of TetR and plasmids inside the cell.

$$R = \frac{R_{tot} - 2D_{tot}}{2C_0} - \frac{1}{2C_1} + \sqrt{\left(\frac{R_{tot} - 2D_{tot}}{2C_0} - \frac{1}{2C_1}\right)^2 + \frac{R_{tot}}{C_0\, C_1}} \tag{3}$$
$$P = \left(1 + C_1\, R\right)^{-2}$$

where $C_0 = \left(1 + K_T\, T\right)^2$ and $C_1 = K_0 + 2\, K_1\, K_T\, T + K_2\, \left(K_T\, T\right)^2$. For the total amount of aTc inside the cell T_{in} we obtain:

$$T_{in} = T + R\left[C_0 - 1 + (K_T T)^2\right] + \frac{2D_{tot}\,R}{1 + C_1\,R}\left[C_1 - K_0 + K_2\,(K_T T)^2\right] \qquad (4)$$

Inverting (4) gives $T(T_{in})$ and from (3) we obtain $R(T_{in})$ and $P(T_{in})$. In supplementing Figure 3 we plot $T(T_{in})$ and $P(T_{in})$ using parameter values from (Table 1).

Equations (2)-(4) relate $RNA(t)$ to the time evolution of T_{in}. We have assumed the simplest possible dynamics of aTc influx-efflux: after an initial step increase, changes in T_{in} are entirely due to constant efflux of free aTc molecules (T):

$$\frac{\partial T_{in}}{\partial t} = -\mu\, T(T_{in}) \qquad (5)$$

Integration in time of equations (2) and (5) yields $RNA(t)$ and $T_{in}(t)$. Before induction (t<0) we assume that the system is at equilibrium with $T_{in} = 0$. Thus,

$$RNA(t=0) \;=\; \frac{\varsigma}{\gamma} D_{tot}\, P(T_{in}=0) \;=\; \frac{\varsigma}{\gamma}\frac{D_{tot}}{\left[1 + K_0\, R(T=0)\right]^2} \qquad (6)$$

is the background level of RNA inside the cell due to leakiness of the promoter. Immediately after induction ($t>0$) we assume that T_{in} is equal to the inducing concentration (200, 400 and 1000 ng/ml).

The time evolution of RNA concentration reflects the time evolution of the total concentration of inducer inside the cell $T_{in}(t)$ (Supplementing Figure 4). We were able to fit the data using the simplest possible scenario of aTc influx-efflux: instantaneous influx and constant effective efflux.

Table 1: Parameter values used to fit the data.

Name	**Description**	**Note**
$V = 6.65 \times 10^{-16}$ L	Cell volume	Radius ≅ 0.46μm, Length ≅ 1μm
$\gamma = 0.0043$ sec^{-1}	RNA degradation rate	From this work (Fig. 3, main text)
$\varsigma = 0.117$ sec^{-1}	Transcription rate	≅ 47 nucleotides/sec
$\mu = 0.0028$ sec^{-1}	aTc efflux	
$K_0 = 10^{11}$ M^{-1}	R-O affinity	Value from (2)
$K_1 = 10^{8}$ M^{-1}	RT-O affinity	Value from (2)
$K_2 = 10^{3}$ M^{-1}	RT_2-O affinity	Value from (2)
$K_T = 2.685\times10^{9}$ M^{-1}	R-T affinity	(3) quotes 9.8×10^{11} M^{-1} for affinity in the presence of Mg^{2+} and 6.5×10^{7} M^{-1} without Mg^{2+}.

D_{tot} = 49 molecules	Number of plasmids	(4) quotes between 50 and 70 copies
R_{tot} = 85 dimmers	Number of TetR dimmers	It has been shown (4) that the total number of TetR repressors in a DH5αPRO cell is around 7000. TetR binds nonspecifically to chromosomal DNA. Due to this weak non-specific binding, we expect the effective concentration of repressors to be much lower, about 1% of the total concentration.

References

1. Le, T. T., Harlepp, S., Guet, C. C., Dittmar, K., Emonet, T., Pan, T. & Cluzel, P. (2005) *Proc Natl Acad Sci U S A*.
2. Lederer, T., Takahashi, M. & Hillen, W. (1995) in *Anal Biochem*, Vol. 232, pp. 190-6.
3. Scholz, O., Schubert, P., Kintrup, M. & Hillen, W. (2000) in *Biochemistry*, Vol. 39, pp. 10914-20.
4. Lutz, R. & Bujard, H. (1997) in *Nucleic Acids Res*, Vol. 25, pp. 1203-10.

Supplementing figure captions

Supplementing figure 1 Fluorescent correlation spectroscopy experimental set-up. The incident excitation solid blue laser beam (Sapphire 488nm, 20mW, Coherent) is expanded and focused onto a diffraction-limited spot on the sample. The green emitted fluorescence is collected in a confocal geometry and detected with a photon counting module (spcm-aqr-16fc, Perkin Elmer). The fluorescent signal is analyzed in real-time with a fast correlator (ALV 5000EPP) to measure the concentration and diffusion coefficient of fluorescent molecules in the detection volume. Dark-field illumination is used to position *E. coli* cells onto the laser beam. Dichroic mirror 1 (XF2037), dichroic mirror 2 (XF2016), long pass filter (XF3085) (Omega Optical, Inc.). Objective lens,100X

oil immersion, 1.3 numerical aperture (Olympus). Focusing lens, achromatic doublet lens, fl 25mm (LAC 181-A, Thorlabs, Inc.).

Supplementing figure 2 Transcription of *ms2* gene from a *tet* inducible promoter in one *E. coli* cell. (A) Autocorrelation functions (normalized to $1/N_o$ on y-axis) of MS2-GFP proteins at several time intervals after induction, t=0min (black), t=30min (light grey), t=50min (grey), and t=70min (dark grey). (B) ms2-RNA concentration as a function of time after induction. The ζ_{free} and ζ_{bound} for MS2-GFP in living cells are 1.4 +/- 0.5 ms and 30 +/- 3 ms, respectively. RNA concentration was derived by multiplying the fraction bound of MS2-GFP with the initial number of MS2-GFP molecules in the cell (N_o). The error bars represent the RNA concentration estimation errors.

Supplementing figure 3 Quasi-equilibrium of the promoter region as function of the total concentration of aTc inside the cell. Probability of an open promoter region $P(T_{in})$.

Supplementing figure 4 Intracellular concentration of aTc as a function of time after induction. Blue, green and red correspond to 200, 400 and 1000 ng/ml induction levels of aTc ($T_{in}(t)$). Black is the mutant induced with 400 ng/ml aTc. .

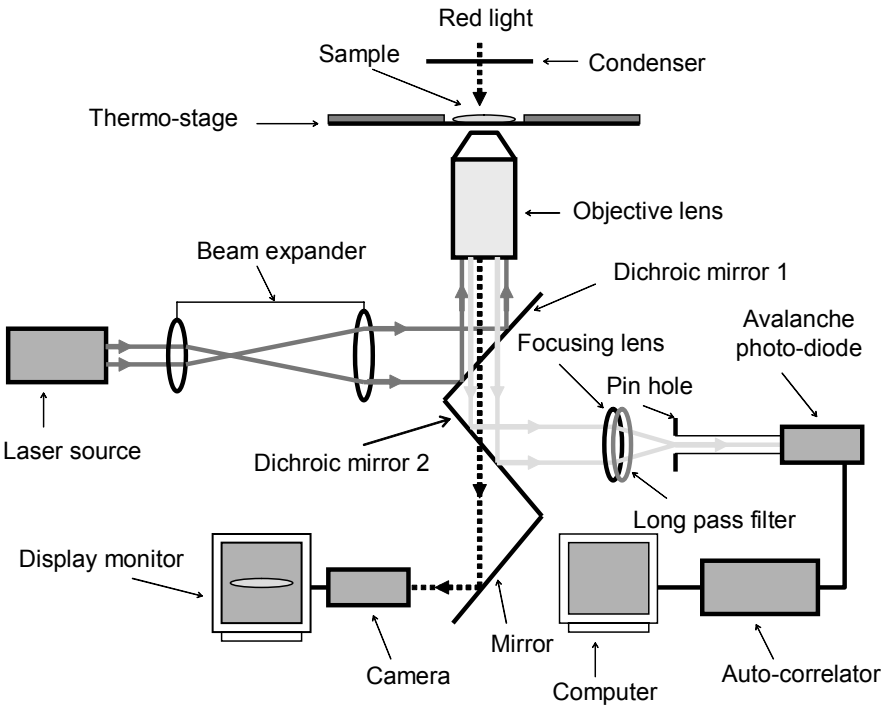

Supplementing figure 1

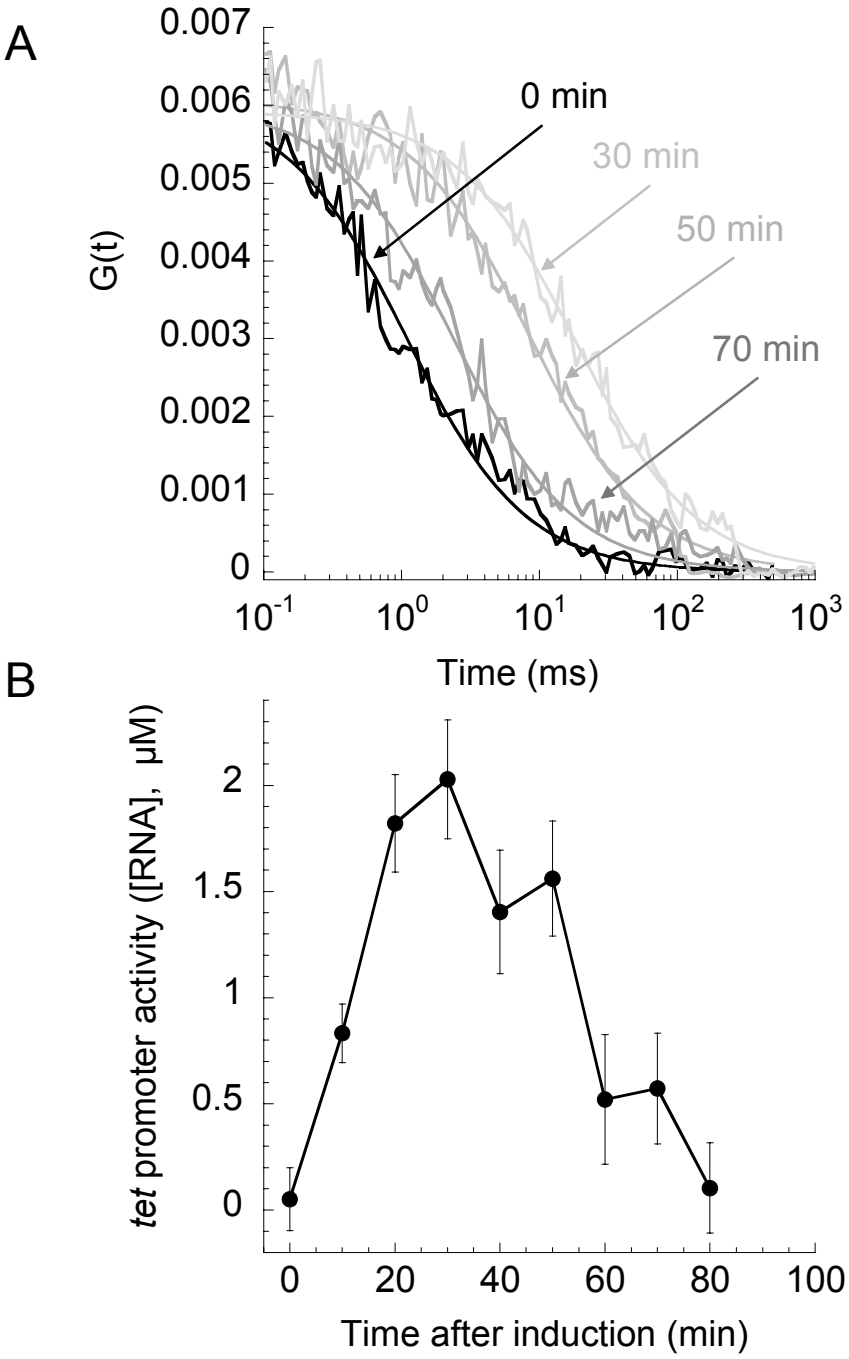

Supplementing figure 2A,B

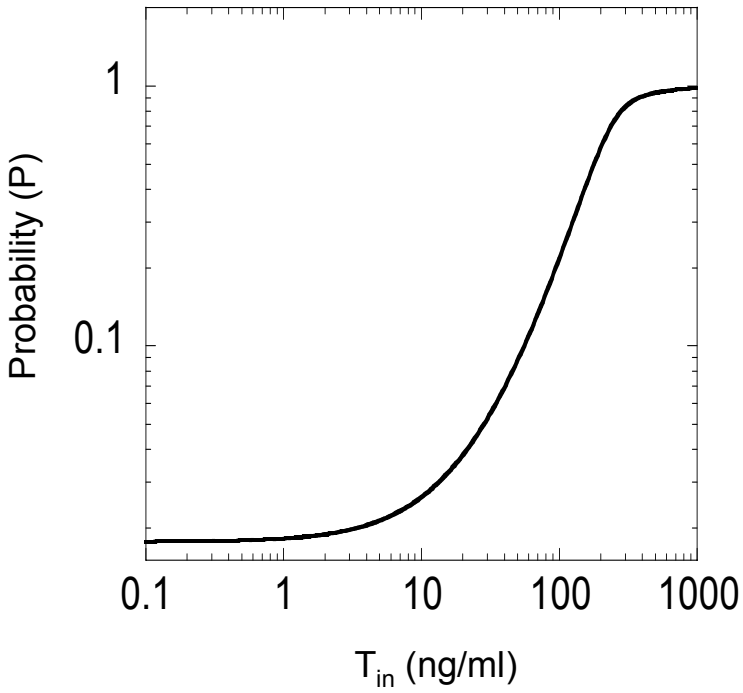

Supplementing figure 3

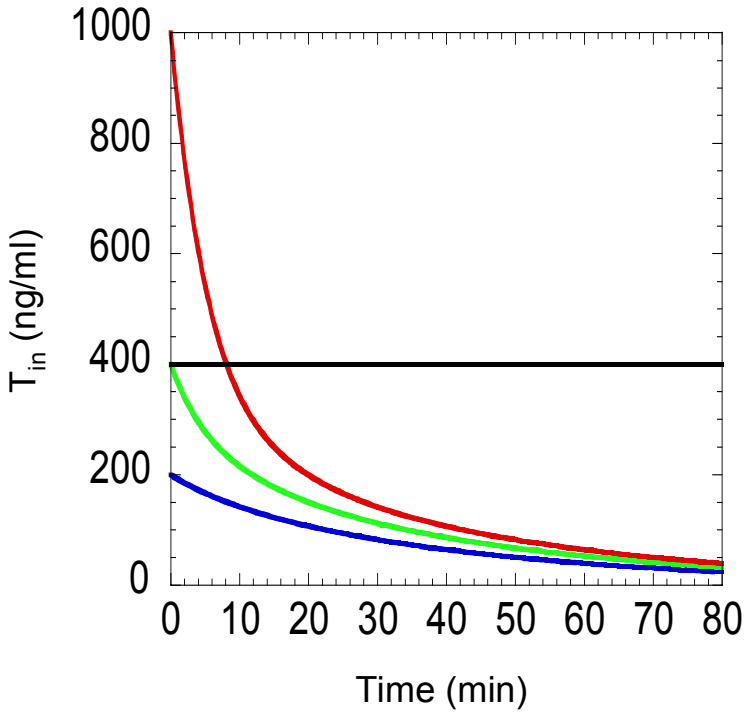

Supplementing figure 4